(7) C. Masters, *J. Chem. Soc., Chem. Commun.*, 1258 (1972).
(8) R. G. Parker and J. D. Roberts, *J. Am. Chem. Soc.*, **92**, 743 (1970).
(9) C. D. M. Beverwijk and J. P. C. M. Van Dongen, *Tetrahedron Lett.*, 4291 (1972).
(10) J. P. C. M. Van Dongen and C. D. M. Beverwijk, *J. Organomet. Chem.*, **51**, C36 (1973).
(11) K. R. Aris, V. Aris, and J. M. Brown, *J. Organomet. Chem.*, **42**, C67 (1972).
(12) G. Rigatti, G. Boccalon, A. Ceccon, and G. Giacometti, *J. Chem. Soc., Chem. Commun.*, 1165 (1972).
(13) H. G. Preston, Jr., and J. C. Davis, Jr., *J. Am. Chem. Soc.*, **88**, 1585 (1966).
(14) H. L. Retcofsky, E. N. Frankel, and H. S. Gutowsky, *J. Am. Chem. Soc.*, **88**, 2710 (1966).
(15) B. F. G. Johnson and J. A. Segal, *J. Chem. Soc., Chem. Commun.*, 1312 (1972).
(16) G. M. Bodner, B. N. Storhoff, D. Doddrell, and L. J. Todd, *Chem. Commun.*, 1530 (1970).
(17) D. E. Axelson, C. E. Holloway, and A. J. Oliver, *Inorg. Nucl. Chem. Lett.*, **9**, 855 (1973).
(18) C. G. Kreiter and M. Lang, *J. Organomet. Chem.*, **55**, 627 (1973).
(19) E. W. Randall, E. Rosenberg, and L. Milone, *J. Chem. Soc., Dalton Trans.*, 1672 (1973).
(20) R. G. Salomon and J. K. Kochi, *J. Organomet. Chem.*, **64**, 135 (1974).
(21) C. A. Tolman, A. D. English, and L. E. Manzer, *Inorg. Chem.*, **14**, 2353 (1975).
(22) J. Evans and J. R. Norton, *Inorg. Chem.*, **13**, 3042 (1974).
(23) L. Garcia, S. I. Shupack, and M. Orchin, *Inorg. Chem.*, **1**, 893 (1962).
(24) P. Schmidt and M. Orchin, *Inorg. Chem.*, **6**, 1260 (1967).
(25) P. D. Kaplan and M. Orchin, *Inorg. Chem.*, **6**, 1096 (1967).
(26) A. R. Brause, F. Kaplan, and M. Orchin, *J. Am. Chem. Soc.*, **89**, 2661 (1967).
(27) P. D. Kaplan, P. Schmidt, and M. Orchin, *J. Am. Chem. Soc.*, **90**, 4175 (1968).
(28) F. Pesa and M. Orchin, *J. Organomet. Chem.*, **78**, C26 (1974).
(29) D. G. Cooper and J. Powell, *J. Chem. Soc., Chem. Commun.*, 486 (1973).
(30) D. Mansuy, J. F. Bartoli, and J. C. Chottard, *J. Organomet. Chem.*, **73**, C39 (1974).
(31) R. Lazzaroni and C Veracini, *J. Organomet. Chem.*, **33**, 131 (1971).
(32) T. Kinugasa, M. Nakamura, H. Yamada, and A. Saika, *Inorg. Chem.*, **7**, 2649 (1968).
(33) M. I. Gel'fman, N. M. Karpinskaya, and V. V. Razumouskii, *Russ. J. Inorg. Chem. (Engl. Transl.)*, **15**, 1438 (1970).
(34) J. Ashley-Smith, I. Douek, B. F. G. Johnson, and J. Lewis *J. Chem. Soc., Dalton Trans.*, 1776 (1972).
(35) C. E. Holloway, G. Hulley, B. F. G. Johnson, and J. Lewis, *J. Chem. Soc. A*, 1653 (1970).
(36) R. Mason and G. B. Robertson, *J. Chem. Soc. A*, 492 (1969).
(37) E. Benedetti, P. Corradini, and C. Pedone, *J. Organomet. Chem.*, **18**, 203 (1969).
(38) W. McFarlane, *Q. Rev., Chem. Soc.*, **23**, 187 (1969).
(39) M. H. Chisholm, H. C. Clark, L. E. Manzer, and J. B. Stothers, *Chem. Commun.*, 1627 (1971).
(40) T. R. Jack and J. Powell, *Inorg. Chem.*, **11**, 1039 (1972).
(41) J. Bordner and D. W. Wertz, *Inorg. Chem.*, **13**, 1639 (1974).
(42) F. R. Hartley, *Chem. Rev.*, **73**, 163 (1973).
(43) E. Ban, R. P. Hughes, and J. Powell, *J. Organomet. Chem.*, **69**, 455 (1974).
(44) A preliminary communication concerning these results has already appeared.[4]
(45) Although up to this point in this paper we have considered $\Delta\delta_C$ in analyzing the effect of olefin coordination, we have found in the case of the styrene complexes that δ_C of the olefinic carbons gave better σ_p^+ correlations[46] than does $\Delta\delta_C$ (see ref 4 for $\Delta\delta_C$ vs. σ^+ plots). The reason for this can be found in the fact that the mechanisms of interaction between the olefinic carbons and the para Y substituent for the coordinated and free styrenes[47] are considerably different.
(46) H. C. Brown and Y. Okamoto, *J. Am. Chem. Soc.*, **80**, 4328 (1958).
(47) G. K. Hamer, I. R. Peat, and W. F. Reynolds, *Can. J. Chem.*, **51**, 897 (1973).
(48) All the ^{13}C NMR and infrared data for complexes **7**–**9** gave considerably better linear correlations when plotted against Brown's σ_p^+ parameters as compared to those using Hammett σ_p values.
(49) G. J. Ray, R. J. Kurland, and A. K. Colter, *Tetrahedron*, **27**, 735 (1971).
(50) J. Hiraishi, *Spectrochim. Acta, Part A*, **25**, 749 (1969).
(51) J. R. Holder and N. C. Baenziger, *J. Am. Chem. Soc.*, **77**, 4987 (1955).
(52) Crystals of the complex *trans*-$[(p\text{-}NO_2C_6H_4CH{=}CH_2)PtCl_2(NC_5H_4Me)]$ proved to be unsatisfactory for x-ray analysis.[53]
(53) S. C. Nyburg, K. Simpson, and W. Wong-Ng, *J. Chem. Soc., Dalton Trans.*, in press.
(54) F. A. Cotton, J. N. Francis, B. A. Frenz, and M. Tsutsui, *J. Am. Chem. Soc.*, **95**, 2483 (1973).
(55) For a more complete discussion of the x-ray structural studies of these styrene–platinum complexes see ref 53.
(56) K. Konya, T. Fujita, H. Kido, and K. Saito, *Bull. Chem. Soc. Jpn.*, **45**, 2161 (1972).
(57) J. R. Roy and M. Orchin, *J. Am. Chem. Soc.*, **81**, 305 (1959).
(58) F. Sartori, L. Leoni, R. Lazzaroni, and P. Salvadori, *J. Chem. Soc., Chem. Commun.*, 322 (1974).
(59) Attempts to prepare the complexes $[(\eta^2\text{-}1,3\text{-diene})PtCl_2(NC_5H_4Me)]$ (1,3-diene = butadiene, isoprene, *cis*- and *trans*-1,3-pentadiene, and *trans,trans*-2,4-hexadiene) yield the dinuclear complexes $(\eta^4\text{-}1,3\text{-diene})[PtCl_2(NC_5H_4Me)]_2$ as insoluble products.
(60) M. G. B. Drew, S. M. Nelson, and M. Sloan, *J. Chem. Soc., Dalton Trans.*, 1484 (1973).
(61) T. G. Hewitt and J. J. DeBoer, *J. Chem. Soc., A*, 817 (1971).
(62) M. Kadonaga, N. Yasuoka, and N. Kasai, *Chem. Commun.*, 1597 (1971).
(63) K. Okamoto, Y. Kai, N. Yasuoka, and N. Kasai, *J. Organomet. Chem.*, **65**, 427 (1974).
(64) R. P. Hughes and J. Powell, *J. Organomet. Chem.*, **60**, 409 (1973).
(65) J. K. Crandall and S. A. Sojka, *J. Am. Chem. Soc.*, **94**, 5084 (1972).
(66) M. C. Caserio, *Sel. Org. Transform.*, **1**, 259 (1970).
(67) T. L. Jacobs and R. C. Kammerer, *J. Am. Chem. Soc.*, **96**, 6213 (1974).
(68) D. Garrett and G. Schmidt, private communication.
(69) We have no explanation for the apparently anomalous behavior of $CH_2{=}CHCH_2OH$.
(70) G. C. Levy and G. L. Nelson, "Carbon-13 Nuclear Magnetic Resonance for Organic Chemists", Wiley-Interscience, New York, N.Y., 1972.
(71) T. Yonemoto, *J. Magn. Reson.*, **12**, 93 (1973).

Contribution from the Department of Chemistry,
The University, Leicester LE1 7RH, England

Single-Crystal Vibrational Spectrum of Bis(dimethyl sulfoxide)dichlorocopper(II) and Infrared Spectra of Some Hexakis(dimethyl sulfoxide) Complexes

DAVID M. ADAMS* and WILLIAM R. TRUMBLE

Received February 3, 1976

AIC60080P

All of the skeletal internal modes of $CuCl_2(DMSO)_2$ have been assigned from the evidence of single-crystal ir and Raman spectra at liquid nitrogen temperature. $\nu(Cu\text{–}O)_s$, $\nu(Cu\text{–}O)_a$, $\nu(Cu\text{–}Cl)_s$, and $\nu(Cu\text{–}Cl)_a$ are at 481, 496, 229, and 286 cm^{-1}, respectively. An outline assignment is given for ir (powder) data for $[M(DMSO)_6]^{2+}$ types.

Introduction

Most studies of the vibrational spectra of inorganic coordination complexes are of dissolved or polycrystalline samples. Data are usually incomplete and, where complex polyatomic ligands are involved, assignments are chiefly restricted to metal–ligand stretching modes. The spectra of powder samples (usually obtained at ambient temperature only) also generally show substantially fewer than the number of bands predicted by factor group analysis (fga) thereby inviting oversimple assignments.

In this paper we report a single-crystal ir and Raman study at liquid nitrogen temperature of $CuCl_2(DMSO)_2$ and its

Table I. Raman Band Positions and Intensities (Arbitrary Units) at Liquid Nitrogen Temperature for $Cu(DMSO)_2Cl_2$ and Related Compounds

$Cu(DMSO)_2Cl_2$					$Cu(DMSO\text{-}d_6)_2Cl_2$						
ν/cm^{-1}	A_g $z(xx)y$	B_{1g} $z(yx)y$	B_{2g} $z(xz)y$	B_{3g} $z(yz)y$	ν/cm^{-1}	A_g $z(xx)y$	B_{1g} $z(yx)y$	B_{2g} $z(xz)y$	B_{3g} $z(yz)y$	$Cu(DMSO)_2Br_2$[a] ν/cm^{-1}	Assignment[b]
42				3							Lattice modes
47		5									
54			5		51			15			
62	30	100	5	3	58	15	45				
74		200	10	6	72		100			64 m	
82	110				78	40				74 w	
85			10		83			25			
108			50		100			50	5		τ_L
110	250	150		12	103	90	50			101 m	
136	70		6		122	20		10			
143				11	134				35 br	128 m, br	δ(CuOS)
148		40	3		142		10				
154	3				147	5					
					157			10 br		163 w	
172			6		174			8 br		177 m	δ(ClCuCl)
182	6	5		9							
188			4								δ(ClCuO)
204				13	204				28	189 vw	
209		10			208		10				
230	130	17	10	4	227	45		5	10	222 m	$\nu(Cu\text{–}Cl)_s$
247	30	20		30						248 w, br	δ(OCuO)/S(SO)[c]
258		40			234		5				
261			25		252			30			
					272	40					
287			8	4	287	2			5		$\nu(Cu\text{-}Cl)_{as}$
314	155	10	10	3						314 w	δ(CSC), a′
345	45	5	5	3	322	10					Ligand
481	170	40	30	5	453	45		20	5	478 m	$\nu(Cu\text{–}O)_s$
691	450	50	40	15	633	80	5	35	10		$\nu(CSC)_s$
727	2	200	5	30	644		35		60		$\nu(CSC)_a$

[a] Powder spectrum. [b] Assignments refer to chloride; equivalences of bromide bands to those of chloride are uncertain. [c] δ(SO)/δ(OCuO) probably coincident for $Cu(DMSO\text{-}d_6)_2Cl_2$.

deuterate. This is used as the basis of further, qualitative, assignments for spectra of $[M(DMSO)_6]^{2+}$ complexes.

The most complete and useful infrared work on DMSO complexes is that of Berney and Weber on $[M(DMSO)_6]^{2+}$ types:[1] their work was to a lower limit of 200 cm^{-1} and was at ambient temperature only. Some Al(III)[2] and Hg(II)[3] complexes of DMSO have been investigated recently by both Raman and ir methods but definitive low-frequency information is lacking in both studies.

Experimental Section

$CuCl_2(DMSO)_2$ was precipitated by mixing ethanolic solutions of $CuCl_2$ and the ligand.[4] Recrystallization from methanol yielded large, green, tabular crystals; axial orientation was determined from x-ray photographs, Figure 1. $CuCl_2(DMSO\text{-}d_6)_2$ and $CuBr_2(DMSO)_2$ were prepared by analogous methods; the bromide was yellow and would not yield large enough crystals for orientational studies. The hexakis(dimethyl sulfoxide) complexes were prepared by the methods of ref 1.

Raman spectra were obtained using Coderg T800 and PhO spectrometers with a Cryocirc cold cell and 514.5-nm excitation from a CRL model 52A laser. For $CuCl_2(DMSO)_2$ power at the sample was restricted to 150 mW to prevent decomposition; for the bromide spectra could only be obtained at liquid nitrogen temperature and with not more than 40 mW at the sample.

Ir spectra were obtained with a Beckman-RIIC FS-720 Fourier spectrometer and an FS7-RF reflectance module, using a wire-grid polarizer. Crystals were examined at near-normal incidence, mounted on a home-made cryostat, using natural faces except for the B_{1u} spectra for which a face was cut and polished normal to *b*. Crystals of the deuteriate were too small for B_{1u} spectra to be obtained.

Results

The data are shown in Tables I and II and illustrated in Figures 2 and 3. Ir reflectance data were analyzed by the Kramers–Kronig method to yield the real and imaginary parts of the complex refractive index $\epsilon = \epsilon' - i\epsilon''$; frequencies quoted are maxima of ϵ''. Considerable sharpening of bands in both ir and Raman spectra was observed upon cooling to liquid nitrogen temperature.

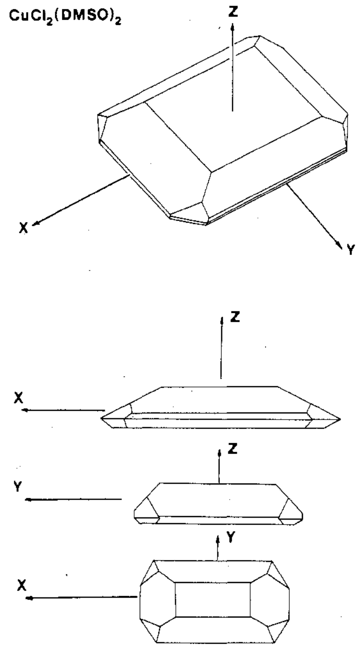

Figure 1. Morphology of $CuCl_2(DMSO)_2$ crystals.

Discussion

$CuCl_2(DMSO)_2$ crystallizes in the orthorhombic group *Pnma* with $Z = 4$. All Cu–Cl bonds lie in *zx* mirror planes with the DMSO ligands located symmetrically on either side.[5]

Table II. Ir Frequencies (cm^{-1}) for Single-Crystal $Cu(DMSO)_2Cl_2$ and $Cu(DMSO\text{-}d_6)_2Cl_2$ Obtained by Kramers–Krönig Analysis of Reflectance Spectra and Corresponding Data for Chloride and Bromide Complexes as Mulls (All Data at Liquid Nitrogen Temperature)

$Cu(DMSO)_2Cl_2$				$Cu(DMSO\text{-}d_6)_2Cl_2$			$Cu(DMSO)_2$-	
Mull	B_{1u} (*z*)	B_{2u} (*y*)	B_{3u} (*x*)	Mull	B_{2u} (*y*)	B_{3u} (*z*)	Br_2 Mull	Assignment[a]
	46 w						50 mw	Lattice modes
75 s	74 m	73 vw	70 s	69 w	68 w	65 m	65 m	
85 m			85 s	78 s		86 w	78 w	
104 s	99 w		103 vs	103 s		99 vs	98 m	τ(ligand)
			147 vs	146 s		141 vs	118 m	$\delta + \pi$(CuOS), $\delta + \pi$(ClCuO) (see text)
150 vs, br		159 vs		156 s	152 m		133 s	
173 m	175 w			170 m			152 m	
				186 w, sh			160 w, m	
198 mw		202 vw		206 m	205 w		172 w	
228 s			228 m	228 s	227 w	226 s	215 s	$\nu(Cu\text{–}Cl)_s$
252 vs	254 w	254 w	248 w	239 sh			248 vs	δ(OCuO)/δ(SO)
				265 w		265 vw	309 w	δ(SO)/γ(SO)
286 vs	286 vs		286 m	287 s	280 vw	288 w		$\nu(Cu\text{–}Cl)_a$
310 m		314 vw					318 w	δ(CSC), a′
343 s	339 w		339 w	322 m		323 w	340 vs	δ(SO)/γ(SO)
485 m			483 vw	454 m		452 vw	474 w	$\nu(Cu\text{–}O)_a$/δ(SO)
500 s		496 m		467 s	468 w		493 s	$\nu(Cu\text{–}O)_a$, b_2

[a] Assignments refer to chloride; equivalences of bromide bands with those of chloride are uncertain. [b] δ(OCuO)/δ(SO) coincident for $Cu(DMSO\text{-}d_6)_2Cl_2$.

Table III. Factor Group Analysis for $CuCl_2(DMSO)_2$[a]

						Internal coordinates		Activities	
D_{2h}^{16}	N_{opt}	N_L	*T*	*R*	N_{int}	ν(Cu–Cl)	ν(Cu–O)	Ir	Raman
A_g	36	24	2	1	9	2	1		x^2, y^2, z^2
B_{1g}	33	24	1	2	6	0	1		xy
B_{2g}	36	24	2	1	9	2	1		xz
B_{3g}	33	24	1	2	6	0	1		yz
A_u	33	24	1	2	6	0	1		
B_{1u}	35	24	1	1	9	2	1	z	
B_{2u}	32	24	0	2	6	0	1	y	
B_{3u}	35	24	1	1	9	2	1	x	

[a] Key: N_{opt}, total number of optic branch modes ($3N - 3$); N_L, internal modes of DMSO; *T*, optic branch translatory modes; *R*, rotatory modes; N_{int}, coupled skeletal modes of the four molecules in the cell.

Table IV. Approximate Mode Description and Summary Assignment for Skeletal Modes of $CuCl_2(DMSO)_2$

Molecule (C_{2v})[a]		Site C_s (*zx*)	Crystal D_{2h}^{16}							
a_1 $\nu(Cu\text{-}O)_s$	ν_1			ν_1	ν_2	ν_3	ν_4	ν_5, ν_6	ν_7, ν_8	ν_9
b_1 $\nu(Cu\text{–}Cl)_a$	ν_2		A_g	481		230		247, 182	154, 136	110
a_1 $\nu(Cu\text{–}Cl)_a$	ν_3		B_{2g}	481	287	230	172	188	148, 136	108
a_1 π(ClCuCl)	ν_4									
a_1 π(OCuO)	ν_5	$9A' \xrightarrow{\times 4}$	B_{1u}		286		175	254		99
b_1 δ(ClCuO)	ν_6		B_{3u}	483	286	228		248	147	103
b_1 δ(CuOS)	ν_7		Av	482	286	230	173	250, 185	150, 136	105
a_1 π(CuOS)	ν_8									
b_1 torsion	ν_9									
b_2 $\nu(Cu\text{–}O)_a$	ν_{10}			ν_{10}	ν_{11}, ν_{12}	ν_{13}, ν_{14}	ν_{15}			
a_2 δ(ClCuO)	ν_{11}		B_{1g}		247, 209	182, 148	110			
b_2 δ(ClCuO)	ν_{12}	$6A'' \xrightarrow{\times 4}$								
a_2 δ(CuOS)	ν_{13}		B_{3g}		247, 204	182, 143	110			
b_2 π(CuOS)	ν_{14}		B_{2u}	496	254, 202	159				
a_2 torsion	ν_{15}		Av	496	249, 205	182, 150	110			

[a] The C_{2v} labels apply only for CuO_2Cl_2 skeletal modes and are a guide only. δ and π indicate motions relative to the plane in which the CuO_2Cl_2 atoms would lie if the molecule were square planar.

Coordination at copper is distorted square planar: the $CuCl_2O_2$ part is close to C_{2v} symmetry but inclusion of the other atoms of DMSO reduces this to C_s. Description of the skeletal modes in terms of C_{2v} labels is therefore no more than a guide. It follows that for each molecule on its C_s crystal site coincident ir and Raman spectra are expected, with no forbidden modes. Correlation coupling of these modes from the four molecules in the cell will yield groups of ir/Raman bands at similar frequencies, their separations reflecting the strength of the correlation field.

In this study we are concerned only with skeletal modes, as the vibrational spectrum of DMSO itself is thoroughly understood from two concordant works, including normal-coordinate analyses,[6,7] and its equivalent vibrations when complexed have been discussed earlier.[1] An fga of the unit cell of $CuCl_2(DMSO)_2$ is shown in Table III and a correlation scheme in Table IV; this scheme was obtained by subtracting ν(S=O), $a_1 + b_2$, from the skeletal representation, $6\ a_1 + 2\ a_2 + 3\ b_1 + 4\ b_2$, and adding the two torsions of the DMSO ligands about the Cu–O bonds, $a_2 + b_1$.

Ligand Modes. The only internal modes of DMSO below 600 cm^{-1} are at 308, 333, and 384 cm^{-1} and are due to δ(CSC), γ(SO), and δ(SO), respectively; location of their equivalents in the complexed state is nontrivial. It is clear that

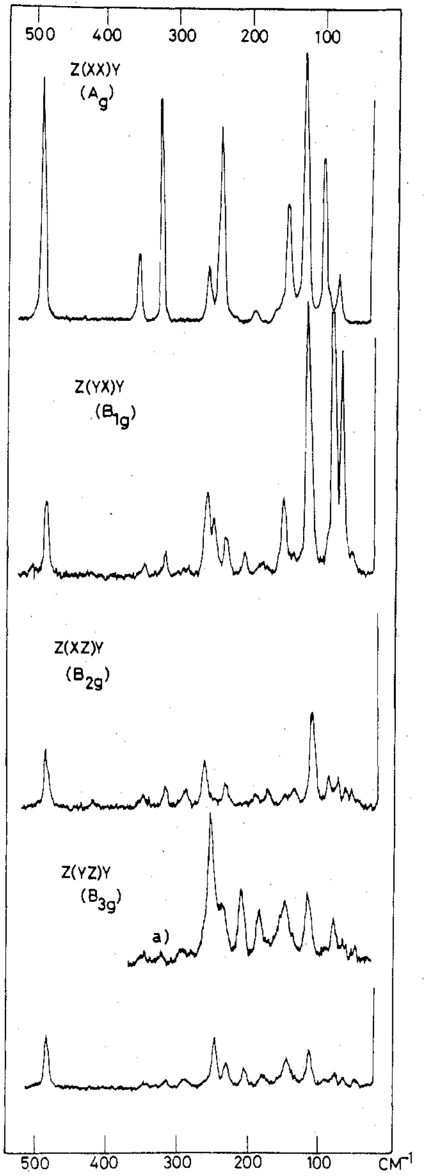

Figure 2. Single-crystal Raman spectra of $CuCl_2(DMSO)_2$ at liquid nitrogen temperature.

the ligand bands at 669 and 697 cm^{-1} due to $\nu(CSC)_s$ and $\nu(CSC)_a$ are at 692 and 730 cm^{-1}, respectively, in the complex, suggesting that all ligand modes may rise. Of the three modes below 400 cm^{-1}, that due to $\delta(CSC)$ is the most distant from the site of coordination and is unlikely to be significantly altered in frequency; we identify it with a Raman band at 314 cm^{-1} which is intense in A_g, consistent with the band origin in a′ of the ligand. Hence, this mode also shows a rise on complex formation. The remaining modes, $\delta(SO)$ and $\gamma(SO)$, are likely to be more significantly affected by coordination: one is clearly ca. 344 cm^{-1} in both ir and Raman spectra but the evidence for the second one is equivocal. We follow Berney and Weber[1] in placing it near 260 cm^{-1} as there is no reasonable alternative.

Metal-Ligand Stretching Modes. Prominent ir and Raman bands in the 480-500-cm^{-1} region are present in the spectra of $CuCl_2(DMSO)_2$ but absent from the ligand spectra: they are lowered ca. 30 cm^{-1} on deuteration. Equivalent bands in hexakis(dimethyl sulfoxide) complexes[1] are highly metal sensitive. We therefore assign them to $\nu(Cu-O)$ modes. According to the correlation scheme the molecular $\nu(Cu-O)_a$ mode should appear in the ir spectra only in B_{2u} and in the Raman spectra in B_{1g} and B_{3g}. It is thereby uniquely identified with the ir band at 496 cm^{-1}: the Raman components are vanishingly weak.

$\nu(Cu-O)_s$ is allowed in the ir spectra in B_{1u} (vanishingly weak) and B_{3u} (483 cm^{-1}) and in Raman spectra at 481 cm^{-1} ($A_g + B_{2g}$). The factor group splitting is within experimental error, reflecting the fact that the Cu-O bonds are buried well within each complex molecule and cannot interact.

$\nu(Cu-Cl)_a$ and $\nu(Cu-Cl)_s$ molecular modes should *both* yield ir components in B_{1u} and B_{3u} and Raman components in A_g and B_{2g}. The evidence is consistent with the behavior of bands at 286 and 228 cm^{-1}, respectively: both are insensitive to deuteration. The higher band is not present in spectra of $CuBr_2(DMSO)_2$, confirming its origin. We note that the B_{2u} band at 254 cm^{-1} cannot be a metal-halogen mode as it has the wrong symmetry. $\nu(Cu-Cl)_s$ is present in Raman (A_g) spectra as an intense band at 230 cm^{-1}.

Lattice Modes. Before an assignment can be attempted for the many deformational modes, it is important to identify the lattice modes so that the *number* of bands of deformational origin can be determined. Fga shows that each of the ir spectra should show two lattice modes: accordingly we attribute 69, 85 cm^{-1} in B_{3u} and 46, 71 cm^{-1} in B_{1u} to this origin, noting that the two rotatory modes expected in B_{2u} are vanishingly weak. It is clear that the ir bands at ca. 100 cm^{-1} are due essentially to internal modes of the molecules (although there will be considerable interaction between these and the lattice modes). The Raman spectra show bands in the same region: in particular the B_{1g} spectrum shows the predicted three at 47, 62, and 74 cm^{-1}.

The Deformational Modes. We have now established that the narrow region from 100 to 260 cm^{-1} contains the many complex deformational modes of $CuCl_2(DMSO)_2$. Location of $\nu(Cu-O)$ and $\nu(Cu-Cl)$ modes indicates that OCuO and ClCuCl deformations may be expected not lower than 240 and 140 cm^{-1}, respectively, if the usual relations hold.

Deformational modes of a_2 and b_2 molecular origin can be present in ir spectra only in the B_{2u} species (see correlation scheme): they are uniquely identified with bands at 159 (s), 202 (vw), and 254 (w) cm^{-1}. The B_{1g} and B_{3g} Raman spectra also show bands near these positions (as required by theory) but, in addition, show further emission at ca. 110 and 185 cm^{-1} which has no ir counterpart. Since $\nu(Cu-O)_a$ has already been located, it is necessary to identify a total of five regions of vibration to complete the a_2, b_2 mode assignment; the ir and Raman evidence, taken together, reveals exactly the number required.

Deformational modes of a_1 and b_1 molecular origin were identified by analogous arguments from the B_{1u}, B_{3u}, A_g, and B_{2g} spectra. Again, exactly the theoretical number of regions was found, i.e., six (since the metal-ligand modes are already known): ca. 105, 136, 148, 175, 182, and 248 cm^{-1}.

At this point we have obtained all of the information that symmetry arguments can provide. The modes crowded into these narrow intervals must interact substantially, making detailed correlation to internal coordinate sets extremely hazardous. Nevertheless, the differing deuteration sensitivities of these bands suggests that some localization of energy occurs and encourages us to make tentative suggestions as follows. The lowest bands in each of the two sets, those at ca. 108 cm^{-1}, are primarily due to torsions of DMSO about the Cu-O bonds, i.e., ν_8 and ν_{12}. The intense ir band at 175 cm^{-1} (B_{1u}) which is nearly insensitive to deuteration is in the correct region for ν_4, π(ClCuCl). All of the deformations of CuOS angles (ν_5, ν_7, ν_{11}, ν_{15}) are probably associated with the bands at 155, 180 cm^{-1} and at 136, 145 cm^{-1}, while the higher frequency ones (202, 245 cm^{-1}; 186, 245 cm^{-1}) are more likely to have a major component involving bending of M-O bonds.

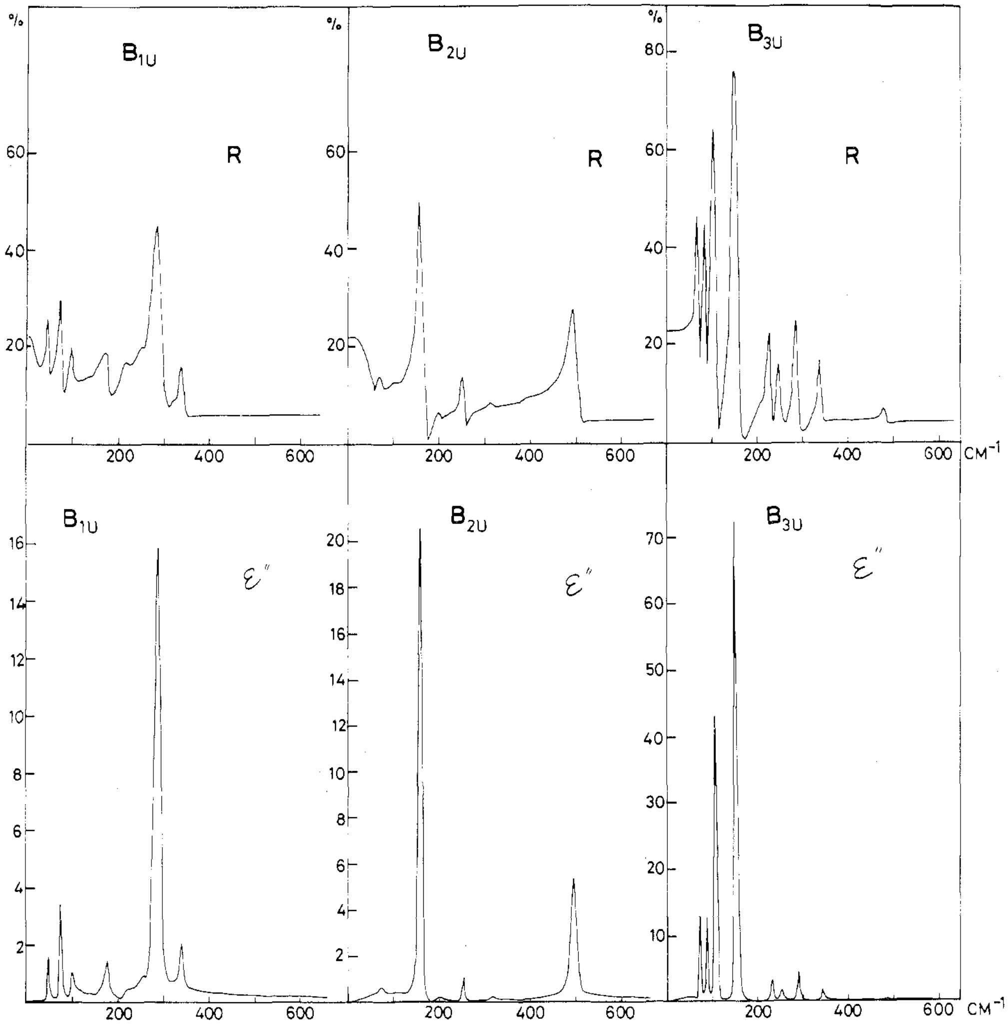

Figure 3. Single-crystal ir spectra of $CuCl_2(DMSO)_2$ at liquid nitrogen temperature showing the experimentally obtained reflectance (R) and the ε'' function obtained from it by Kramers-Krönig analysis.

It is evident from the spectra and our interpretation of them that there are spectral regions corresponding to every one of the molecular internal modes, including the complex deformations and torsions created by attaching DMSO to the metal. Assignment of the metal–ligand modes has been placed on a firmer foundation and an ambiguity relating to ν(Cu–Cl) removed.

Hexakis(dimethyl sulfoxide) Complexes. No single-crystal x-ray structure has been reported for a hexakis(dimethyl sulfoxide) complex. However, many hexakis complexes $[ML_6]A_2$ (where L = imidazole[8] or pyridine *N*-oxide;[9-11] $A^- = ClO_4^-$, NO_3^-, or BF_4^-), adopt the space group $R\bar{3}$, with $Z = 1$, in which the molecular point group, the site group, and the factor group are all S_6. It is probable that the same structure is adopted for L = DMSO. This conclusion was also reached by Berney and Weber[1] from consideration of the ir behavior of some of the internal modes of DMSO.

Given a unimolecular primitive cell S_6, the ir selection rules are simple, correlating from octahedral symmetry.

$$\begin{array}{lll} & \qquad O_h & \qquad S_6 \\ \begin{array}{l}\nu_3\\ \nu_4\\ \nu_6\end{array} & \begin{array}{l}\left.\begin{array}{l}\nu(\text{M-O})\ t_{1u}\\ \delta(\text{M-O})\ t_{1u}\end{array}\right\}\text{ir active}\\ \delta(\text{M-O})\ t_{2u}\ \ \text{inactive}\end{array} & \left.\begin{array}{l}A_u+E_u\\ A_u+E_u\\ A_u+E_u\end{array}\right\}\text{all ir active}\end{array}$$

In addition there are $3\ A_u + 3\ E_u$ modes involving bending of MOS angles and torsions about the M–O bonds.

Our ir data, Table V, show five regions of absorption of which Berney and Weber[1] saw only the first two. On the basis of our $CuCl_2(DMSO)_2$ assignment and by taking $[Ni(DMSO)_6](ClO_4)_2$ as typical they are attributed as follows: ca. 450 cm^{-1} ν(M–O), ν_3; 250 cm^{-1}, ν_4; 190 cm^{-1}, δ(MOS); 140 cm^{-1}, ν_6; 100 cm^{-1} torsion about M–O; O_h labels are used for convenience.

Table V. Ir Wavenumbers (cm^{-1}) and Assignment for Some Hexakis(dimethyl sulfoxide) Complexes[a]

$[MnL_6]$-$[ClO_4]_2$ LN	$[FeL_6]$-$[ClO_4]_2$ RT	$[NiL_6][ClO_4]_2$ RT	$[NiL_6][ClO_4]_2$ LN	Assignment
60 mw		61 w	69 m	Lattice modes
73 s	88 w	74 sh	89 sh	
114 sh	105 w	98 m	103 m	Torsion
122 s	140 w	132 m	138 m	ν_6
153 sh	190 s	186 m	194 s	δ(MOS)
175 s				
220 vs				ν_4; ligand mode
241 sh	260 s, br	243 s, br	249 s	
258 m			266 sh	
314 s	328 w	318 s	325 s	Ligand
341 s	360 w	344 s	347 s	
418	415	444		ν_3[b]
	438			

[a] LN = liquid nitrogen temperature; RT = room temperature.
[b] Room-temperature data from ref 1.

Acknowledgment. We thank the SRC for a grant to W.R.T.

Registry No. $Cu(DMSO)_2Cl_2$, 14215-41-9; $Cu(DMSO\text{-}d_6)_2Cl_2$, 59491-64-4; $Cu(DMSO)_2Br_2$, 59448-49-6; $[MnL_6][ClO_4]_2$, 16884-55-2; $[FeL_6][ClO_4]_2$, 16742-95-3; $[NiL_6][ClO_4]_2$, 16742-94-2.

References and Notes

(1) C. V. Berney and J. H. Weber, *Inorg. Chem.*, **7**, 285 (1968).
(2) J. Meunier and M. T. Forel, *Spectrochim. Acta, Part A*, **29**, 487 (1973).
(3) P. Biscarini, L. Fusina, and G. D. Nivellini, *J. Chem. Soc., Dalton Trans.*, 1003 (1972).
(4) J. Selbin, W. E. Bull, and L. H. Holmes, *J. Inorg. Nucl. Chem.*, **16**, 219 (1961).
(5) R. D. Willett and K. Chang, *Inorg. Chim. Acta*, **4**, 447 (1970).
(6) W. D. Horrocks and F. A. Cotton, *Spectrochim. Acta*, **17**, 134 (1961).
(7) M. T. Forel and M. Tranquille, *Spectrochim. Acta, Part A*, **26**, 1023 (1970).
(8) A. Santoro, A. D. Mighell, M. Zocchi, and C. W. Reimann, *Acta Crystallogr., Sect. B*, **25**, 842 (1969).
(9) T. J. Bergendahl and J. S. Wood, *Inorg. Chem.*, **14**, 338 (1975).
(10) A. D. Van Ingen Schenau, G. C. Verchoor, and C. Romers, *Acta Crystallogr., Sect. B*, **30**, 1686 (1974).
(11) D. L. Kepert, D. Taylor, and A. H. White, *J. Chem. Soc., Dalton Trans.*, 670 (1973).

Contribution from the Department of Chemistry,
Faculty of Science, Kumamoto University, Kumamoto 860, Japan

Kinetics of the Disproportionation Reaction of Mercury(I) with Hydrogen Cyanide in Acidic Solutions

ISAO SANEMASA

Received November 18, 1975

AIC50828O

The kinetics of the disproportionation reaction of mercury(I) with HCN in perchloric acid solutions have been measured by the stopped-flow method. The rate law is given by $-d[Hg(I)]/dt = 2.2 \times 10^3[Hg(I)][HCN][H^+]^{-1}$ M s^{-1} at 25 °C. The activation parameters are $\Delta H^* = 9.5 \pm 0.2$ kcal mol^{-1}, $\Delta S^* = -11.6 \pm 0.6$ cal mol^{-1} deg^{-1}. The rate constant, k_1, for the possible rate-determining reaction $Hg_2OH^+ + HCN = Hg^0 + HgCN^+ + H_2O$ is calculated to be 2.2×10^8 M^{-1} s^{-1}. The breaking of the Hg–Hg bond is considered to be the rate-determining step in the disproportionation reaction with HCN. Discussions on some possible mechanisms are made.

Introduction

It is generally accepted that the rate of disproportionation of Hg_2^{2+} into Hg^{2+} and dissolved mercury atoms is rapid and is readily reversible[1]

$$Hg_2{}^{2+} \rightleftharpoons Hg^0 + Hg^{2+} \qquad (1)$$

The equilibrium constant, K_d, measured by many workers,[2,3] more recently by Moser and Voigt[4] who gave 5.5×10^{-9} M at 25 °C, shows Hg_2^{2+} is sufficiently stable in acidic solutions.

Many texts describe Hg_2^{2+} as unstable toward disproportionation with ligands which form strong covalent bonds such as ammonia, many amines, cyanide ion, hydroxide ion, thiocyanide ion, sulfide, and acetylacetone.[5] However, no data concerning the kinetics have been reported to the best of our knowledge. The disproportionation reaction of Hg_2^{2+} in the presence of ligands which form stable mercuric complexes has been believed to proceed via eq 1. That is, decreasing the concentration of free mercuric ions with concomitant formation of metallic mercury shifts the equilibrium to the right. However, little information is available to discuss the mechanism in further detail. It is an interesting question whether ligands induce the spontaneous disproportionation as mentioned above or they take part in direct interaction to break the Hg–Hg bond.

This paper describes the kinetics of the disproportionation reaction of Hg_2^{2+} with HCN. The reasons that HCN was chosen were (1) simple interpretation of the kinetic results, i.e., kinetic contribution from the CN^- may be neglected owing to the sufficiently high pK value of HCN, and (2) formation of a very stable mercuric cyanide complex even in acidic solutions.

Experimental Section

Materials. Doubly distilled water was used throughout this work. All the chemicals were of analytical reagent grade unless otherwise specified. Metallic mercury was purified in the usual manner.[6] Stock solution (0.01 M) of mercuric perchlorate was prepared by dissolving the required amount of mercuric oxide (red) in perchloric acid in 0.05 molar excess of this acid. Mercurous perchlorate solutions (10^{-2}–10^{-4} M) were prepared from the mercuric perchlorate solution by dilution with 0.05 M $HClO_4$ and shaking with a few drops of metallic mercury. These solutions were kept over the metallic mercury. The solutions (10^{-2}, 10^{-3} M) thus prepared were standardized by oxidizing the Hg(I) with $KMnO_4$ and titrating the resulting Hg(II) against KSCN with ferric alum indicator. More dilute mercurous sample solutions used in the kinetic measurements were prepared from the 10^{-3} M stock solution by dilution with $HClO_4$ and were not kept in contact with metallic mercury; their concentrations were determined spectrophotometrically based on calibration curves made by the 10^{-4} M stock solution.[6] The acid concentrations of the sample solutions were determined titrimetrically by Na_2CO_3 against methyl red indicator. A KCN stock solution (0.1 M) was prepared. More dilute solutions, 2×10^{-3}–10^{-2} M, were prepared by dilution with water and their concentrations were standardized against $AgNO_3$ with KI indicator. Merck grade $NaClO_4$ was used to examine the effect of ionic strength.

Stoichiometric Measurements. The stoichiometry of the overall reaction of Hg_2^{2+} with HCN was measured by spectrophotometry at 236.5 nm in a stopped-flow apparatus. Stoichiometry with regard to elemental mercury was measured by the atomic absorption method. In the flameless atomic absorption method, the mercury compounds in the solution are reduced with tin(II) chloride, and resulting elemental mercury is driven as a vapor by an air stream into an acidic permanganate absorption solution[7] or a measuring cuvette.[8] In the absence of the reductant, only mercury presented in the elemental state in the solution is driven.[9] This method is, therefore, suitable for the determination of stoichiometry regarding elemental mercury. The apparatus and procedure were essentially similar to those employed by many workers[7,10,11] to concentrate trace amounts of mercury. Two gas-washing type cylindrical vessels of 3-cm diameter and 100-ml capacity, each with a glass-sintered inlet tube, were used. One was used as a reduction–aeration vessel and the other as an absorbing vessel. These vessels were connected to each other and further connected to a nitrogen cylinder through a regulator with polyethylene tubes. The procedure for the stoichiometric measurements of mercury consisted of two steps. In the first step, the sample solution in the reduction–aeration vessel was treated with and without the reductant and was aerated for 30 min by nitrogen gas at constant flow rate, 1.5 l./min, into the absorbing vessel in which 20 ml of a permanganate–sulfuric acid solution was placed. This solution was then decolorized by the dropwise addition of hydroxammonium chloride solution (1.44 M). In the second step, the decolorized solution was diluted to 100 ml with water, a suitable aliquot of which was treated with the reductant, and the resulting mercury was further aerated into the measuring cuvette. The reductant used was a 0.44 M tin(II) chloride solution in 1 M HCl. In the first step, each 1 ml of tin(II) chloride and 18 N sulfuric acid was used as the reductant, whereas each 2 ml of these solutions was used in the second step. The solution used for absorbing mercury was prepared by mixing equal volumes of 0.13 M potassium permanganate and 18 N sulfuric acid. The sample solution was prepared